Contract AF 61(052)-817 1 September 1968

AFCRL-68-0614

AD-681 468

FINAL SCIENTIFIC REPORT

INVESTIGATIONS OF SOME OXIDE CRYSTALS BY ESR AND OPTICAL METHODS

Prof. Dr. B. Elschner

II. Physikalisches Institut
Technische Hochschule Darmstadt
6100 Darmstadt
Hochschulstrasse 2
Germany

This research has been sponsored in part by the European Office of Aerospace Research, OAR, United States Air Force under contract AF 61(052)-817

CONTENTS

Introduction

The results we have got in our work for the contract AF 61(052)-817 have been reported in six Progress Reports and one Scientific Report. This Final Report will give a short summary of these investigations and a more detailed description of those not yet reported.

In detail the following research was done:

1. The mineral Benitoit was investigated by Electron-Spin-Resonance (ESR)[7]. This crystal contains iron ions Fe^{3+} in small percentage. We have written a FORTRAN-Program to compute the constants of the Spin-Hamiltonian from the resonance magnetic fields. It also computes the energy eigenvalues of the Spin-Hamiltonian. These are in good agreement with experiment thus indicating that the right Spin-Hamiltonian was chosen.

2. This program was used to set up the Spin-Hamiltonian of gadolinium ions Gd^{3+} in $YCl_3 \cdot 6\ H_2O$ and of iron ions Fe^{3+} in SnO_2.

3. SnO_2-crystals, both undoped and doped with vanadium ions V^{4+} and iron ions Fe^{3+}, were grown from the vapor phase and investigated by measuring resistivity, optical transmission, and ESR.

4. Ruby-crystals with different concentrations of chromium ions Cr^{3+} were grown with aid of a Verneuil set up [1]. The fluorescence lifetime was measured at various temperatures and concentrations using a sampling technique according to Zarowin [3].

5. Several crystals of the boracite-type were grown with aid of a transport-reaction according to H. Schmid [7] and the optical transmission was analyzed [6]. The ESR-Spectrum of Ni-J-boracite was recorded and interpreted by an effective spin $S_{eff} = 1/2$ [2, 7].

6. A giant pulse LASER was built [2, 7] and frequency doubling of boracites was investigated [4, 5, 7].

7. The magneto-electric effect of Ni-J-Boracite has been measured.

1) Progress Report NO. 1, 22nd July 1965

2) Progress Report NO. 2, 7 April 1966

3) Progress Report NO. 3, 22nd July 1966

4) Progress Report NO. 4, 2 December 1966

5) Progress Report NO. 5, 1st June 1967

6) Progress Report NO. 6 and 7, 14th December 1967

7) Scientific Report NO. 1, 15th March 1967

A. Electron Spin Resonance of Benitoit

A detailed description of our measurements on benitoit $BaTi(SiO_3)_3$ has already been given [1], so that we can restrict ourself to sum up the essential results:

Benitoit minerals are usually found at headwaters of San Benito River, South-California, USA [2]. The crystal structure is described by the space-group D_{3h}^2-C$\bar{6}$c2 [3]. There are two Ba^{2+}- and two Ti^{4+}-ions in the unit cell of the crystal, both arranged on trigonal axes parallel to the c-axis. The sites of the Ti- and Ba-ions are not equivalent, they have different positions relative to a mirror plane perpendicular to the c-axis. The Ba- and Ti-ions are surrounded by six oxygen ions forming an octahedron, that round the Ti^{4+}-ion is almost regular, while that round the Ba^{2+}-ion is axially disturbed.

The ESR investigation gave two spectra of five absorption lines each, indicating that our Benitoit has as impurities ions with S = 5/2 sitting on magnetic non equivalent sites. A X-ray fluorescence spectrum showed that our crystals contained iron impurities. We assumed that the paramagnetic spectrum was due to Fe^{3+} ions sitting on the Ba- and Ti-sites. The ground state of Fe^{3+} is $^6S_{5/2}$, therefore we used a Spin-Hamiltonian for S-state ions in a crystalline field with octahedral symmetry [4]. In our case we obtained for Fe^{3+} ions with S = 5/2 in the benitoit

$$
\begin{aligned}
H = {} & g_{\parallel} \cdot \beta H_o S_z \cos\theta + \tfrac{1}{2} g_{\perp} \beta H_o (S_+ + S_-) \sin\theta \\
& + D\left(S_z^2 - \tfrac{35}{12}\right) - \tfrac{7}{36}(a-F)\left(S_z^4 - \tfrac{95}{14} S_z^2 + \tfrac{81}{16}\right) \\
& + \frac{a\sqrt{2}}{36} \Big\{ e^{i3(\varphi \pm \alpha)} (S_z S_+^3 + S_+^3 S_z) \\
& + e^{-i3(\varphi \pm \alpha)} (S_z S_-^3 + S_-^3 S_z) \Big\}
\end{aligned}
$$

$g_{\parallel}$ = g-factor for magnetic field H_o parallel c-axis
$g_{\perp}$ = g-factor for magnetic field H_o perpendicular c-axis
D, a, (a-F) = crystalline electric field constants
θ = angle between c-axis and magnetic field
φ = azimuth between magnetic field and 100 direction
α = angle of inequivalent sites of Ba- and Ti-ions against the cubic axes of the octahedron

We have written a FORTRAN Program [5], which computes the constants of the Spin Hamiltonian by a trial and error method from the observed transitions. As shown in the table, we have got almost the same values as published independently [6] before our investigations were finished.

	Our Results	Elsewhere Published	
$D(cm^{-1})$	0.03371 ± 0.00002	± 0.03382 ± 0.00003	
$a-F(cm^{-1})$	-0.01170 ± 0.00006	± 0.01187 ± 0.0001	
$a(cm^{-1})$	-0.0136 ± 0.0005	± 0.0123 ± 0.0003	T = 295°K
$g_{\parallel}$	1.9992 ± 0.0005	2.0026 ± 0.0005	spectrum I (strong)
$g_{\perp}$	2.0029 ± 0.0005	2.0026 ± 0.0005	
$D(cm^{-1})$	0.0354 ± 0.0001	± 0.03582	
$a-F(cm^{-1})$	-0.0118 ± 0.0003	± 0.01211	
$a(cm^{-1})$	-0.015 ± 0.003	± 0.01251	T = 77°K
$g_{\parallel}$	1.999 ± 0.002	2.0026	spectrum I (strong)
$g_{\perp}$		2.0026	
$D(cm^{-1})$	0.02449 ± 0.00004	± 0.02448 ± 0.0001	
$a-F(cm^{-1})$	-0.0123 ± 0.0002	± 0.0127 ± 0.0001	
$a(cm^{-1})$			T = 295°K
$g_{\parallel}$	2.005 ± 0.001	1.998 ± 0.001	spectrum II (weak)
$g_{\perp}$	1.999 ± 0.001	1.998 ± 0.001	
$D(cm^{-1})$	0.0263 ± 0.0002		
$a-F(cm^{-1})$	-0.0116 ± 0.0006		
$a(cm^{-1})$	-0.010 ± 0.006		T = 77°K
$g_{\parallel}$	2.004 ± 0.003		spectrum II (weak)
$g_{\perp}$			

The signs of D, a, and (a-F) were determined by a measurement at liquid helium temperature. The first spectrum has a greater constant D, indicating that it belongs to a more disturbed octahedral crystal surrounding. Because it is also about ten times more intensive than the second spectrum, preferently Ba-sites are occupied by the Fe^{3+} ions.

Computing the angle-variation and the energy values as a function of field shows an excellent agreement between theoretical and experimental values. The greatest deviation is about 6.5%. The zero field splittings are given by the following formula:

$$\Delta_{1,2} = D - \frac{3}{2}(a-F) \pm \sqrt{(3D + \frac{a-F}{6})^2 + \frac{20}{9} a^2}$$

We have got the following values for the zero field splitting for T = 300°K:

Ba-site: $\Delta_1 = (0.0500 \pm 0.0002)\ cm^{-1} \hat{=} 1.52$ GHz lying lowest
$\Delta_2 = (0.1525 \pm 0.0002)\ cm^{-1}$

Ti-site: $\Delta_1 = (0.028 \pm 0.001)\ cm^{-1}$ lying lowest
$\Delta_2 = (0.114 \pm 0.001)\ cm^{-1}$

Perhaps benitoit is useful as a MASER at a signal frequency of 1.52 GHz. To decide this, relaxation time measurements are to be made.

1) Our Scientific Report NO. 1, 15th March 1967
2) Min. Res. U. S. für 1909, 911, II, 742
3) Zachariasen, Strukturberichte I, 328; II, 128 and 527
4) Bleaney and Trenham, Proc. Roy. Soc. A, 223, 1 (1954)
5) W.J. Becker, to be published
6) S.P. Burley and G.J. Troup, Brit. J. Appl. Phys. 16, 315 (1965)

B. Electron Spin Resonance of Gd^{3+}:Yttrium Chlorine [1]

Our $Gd^{3+}:YCl_3 \cdot 6H_2O$ crystals were grown from solution. Gd_2O_3 and Y_2O_3 were mixed together in a rate giving one Gd-atom at 600 Y-atoms. The composition reacted with hydrochloric according to the equation

$$Y_2O_3 + 6\ HCl \rightarrow 2\ YCl_3 + 3\ H_2O$$
$$Gd_2O_3 + 6\ HCl \rightarrow 2\ GdCl_3 + 3\ H_2O$$

The reaction takes place during several hours warming and moving the mixture. Having evaporated nearly all water the cristallization occurs in an exsiccator.

We have got monocline crystals, which were very hygroscopic. Therefore they were protected by a polystirol layer. The picture shows a crystal with its three cristallographic axes. The monocline axis b can easily be seen from the form of the crystal. The monocline angle is $\beta = 93.6^{\circ}$ [2].

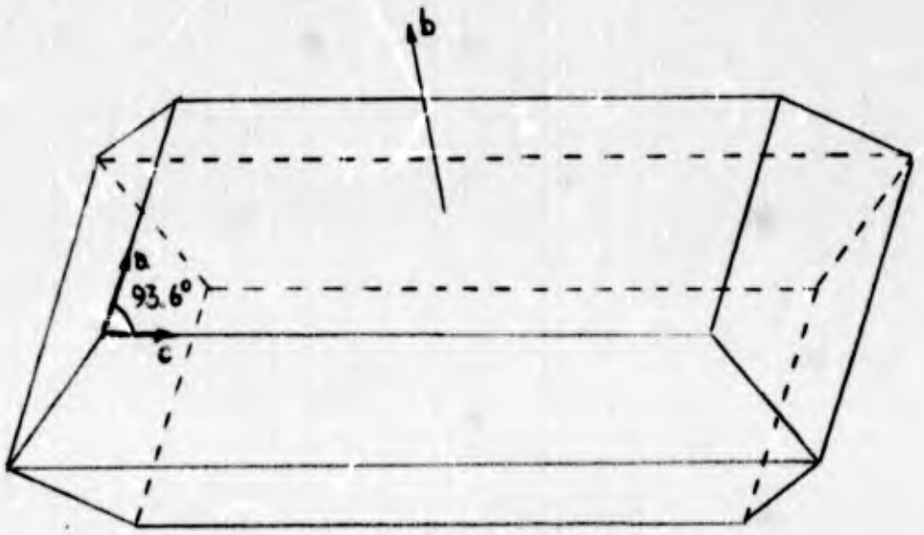

Recording the ESR-spectrum gave seven absorption lines according to the Gd^{3+}-spin S = 7/2. Rotating the crystal round two independent axes showed, that there are three perpendicular magnetic axes. If the magnetic field is parallel to these axes the splitting of the absorption lines is a maximum or minimum. The axis of the smallest splitting is identical with the monocline axis b and is called y-axis.

The two other axes are called x- and z- axis showing maximum splitting. The figure shows the position of the magnetic axes relative to the crystal axes.

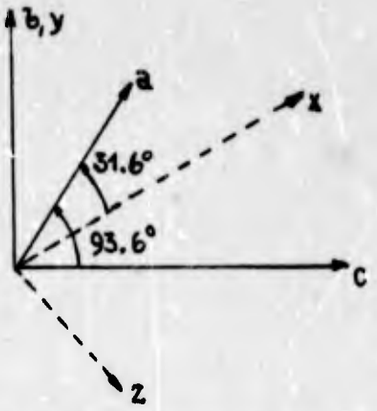

We could describe the spectrum with a Spin-Hamiltonian of the form

$$H = \beta(\vec{H}_o \tilde{g} \vec{S}) + B_2^0 O_2^0 + B_4^0 O_4^0 + B_2^2 O_2^2$$

$\vec{H}_o$ = external magnetic field

$\vec{S}$ = spin operator

$\tilde{g}$ = g-tensor with main axes g_x, g_y, g_z

O_n^m = combination of spin-operators of higher power [3)]

B_n^m = crystal field constants

We chose the z-axis as quantization axis, though it is not the axis with maximum splitting. But all seven transitions could be observed there in contrary to the x-axis, which has maximum splitting. Only five transitions could be observed at the x-axis, because the klystron-frequency (ν = 9430.8 MHz) was too low to observe the remaining two lines. Therefore, we had two more values for our program computing the constants of the Spin-Hamiltonian, if we used the z-axis as quantization axis.

We got the following constants for the Spin-Hamiltonian at a temperature T = 293°K:

$g_x = 1.988 \pm 0.004$ $\qquad$ $3\,B_2^0 = -(0.0534 \pm 0.0005)\ cm^{-1}$

$g_y = 1.993 \pm 0.004$ $\qquad$ $120\,B_4^0 = -(0.0006 \pm 0.0002)\ cm^{-1}$

$g_z = 1.999 \pm 0.004$ $\qquad$ $B_2^2 = (0.0256 \pm 0.0005)\ cm^{-1}$

Using these constants we computed the zero field splittings

$\Delta_1 = 0.257\ cm^{-1}$ lying lowest
$\Delta_2 = 0.236\ cm^{-1}$
$\Delta_3 = 0.372\ cm^{-1}$ lying highest

When we measured the temperature variation of the Spin-Hamilton's constants in the range $80^{\circ}K \leq T \leq 330^{\circ}K$, we got to know, that B_2^0 varied about 12%. The other constants did not change. The sign of B_2^0 was determined by a measurement at $T = 1.2^{\circ}K$.

The following pictures show the angle variation of the spectrum. The computed curves agree with the measured points about 4%. The energy values as a function of applied field are computed, too. The measured resonance-absorptions are marked in the figures. The computed energies could be confirmed by a measurement in the Q-band ($\nu = 35.144$ GHz).

1) D. Meierling et al., to be published

2) M. Mareizo et al., Acta Cryst. 14, 234 (1961)

3) D.A. Jones et al., Proc. Phys. Soc. A74, 249 (1961)

MEASURED AND CALCULATED ANGULAR VARIATION

OF Gd^{3+} IN $YCl_3 \cdot 6H_2O$ IN (Z,Y) PLANE

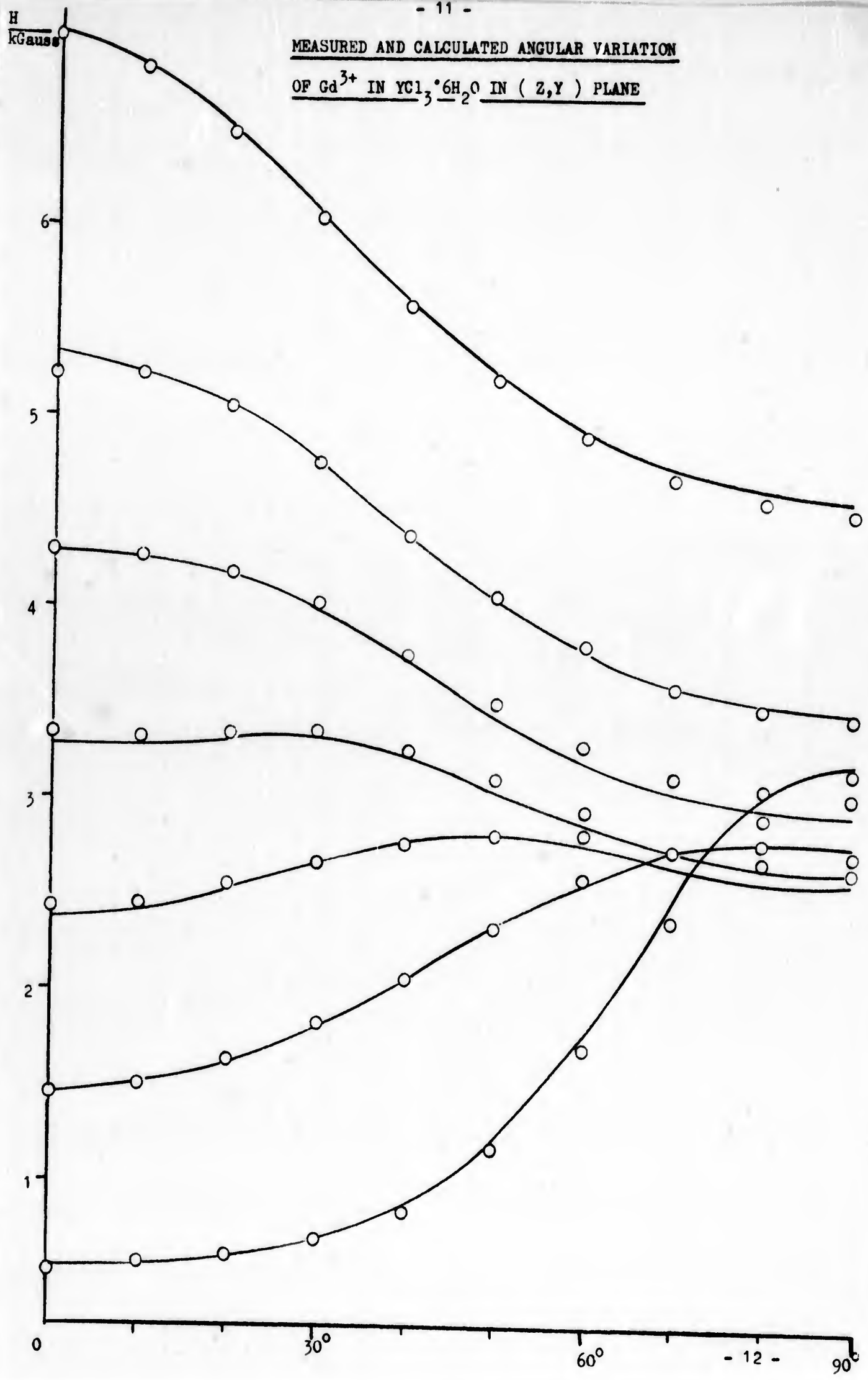

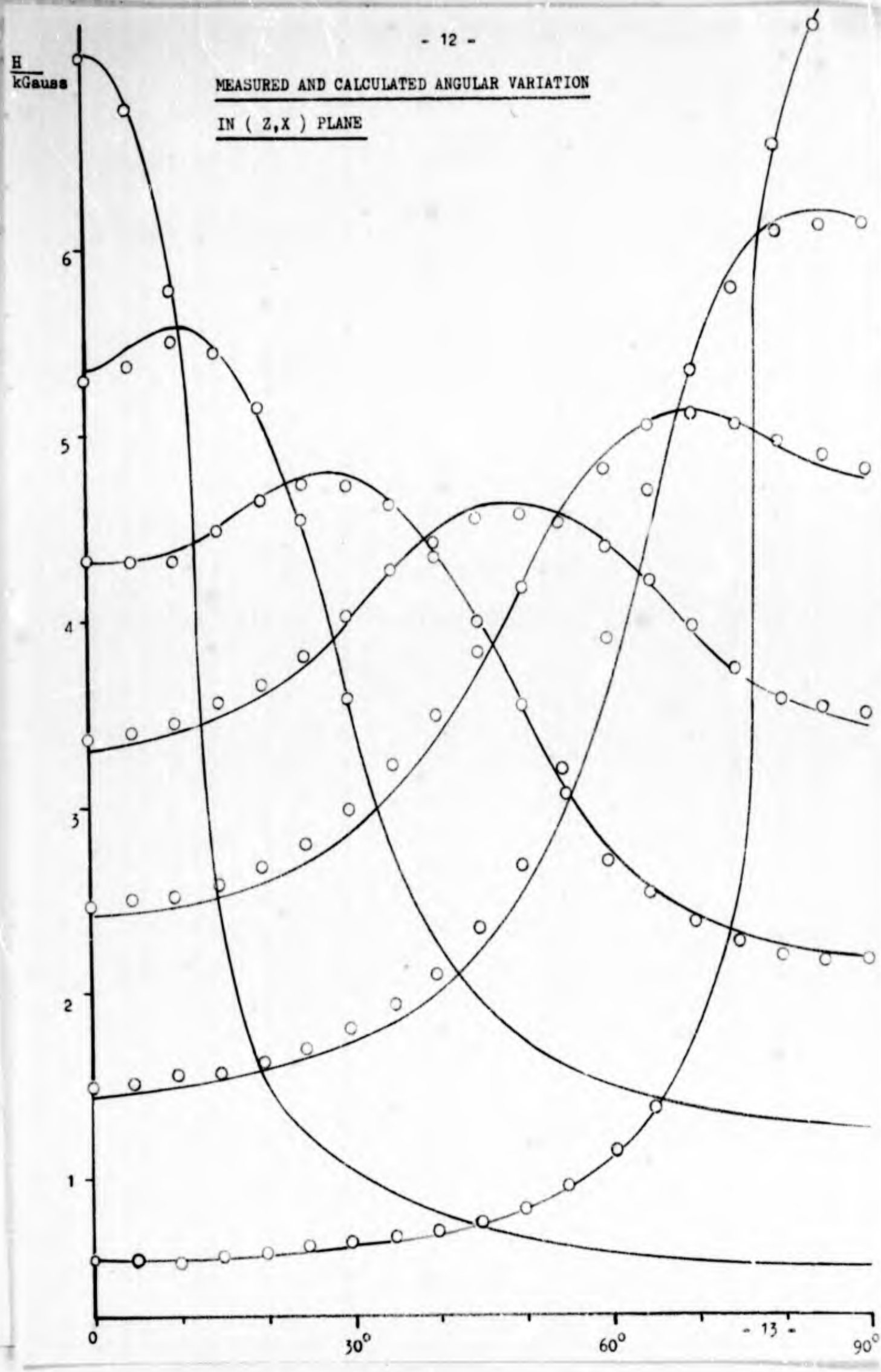
H
kGauss
MEASURED AND CALCULATED ANGULAR VARIATION
IN (Z,X) PLANE
6
5
4
3
2
1
0
30°
60°
90°

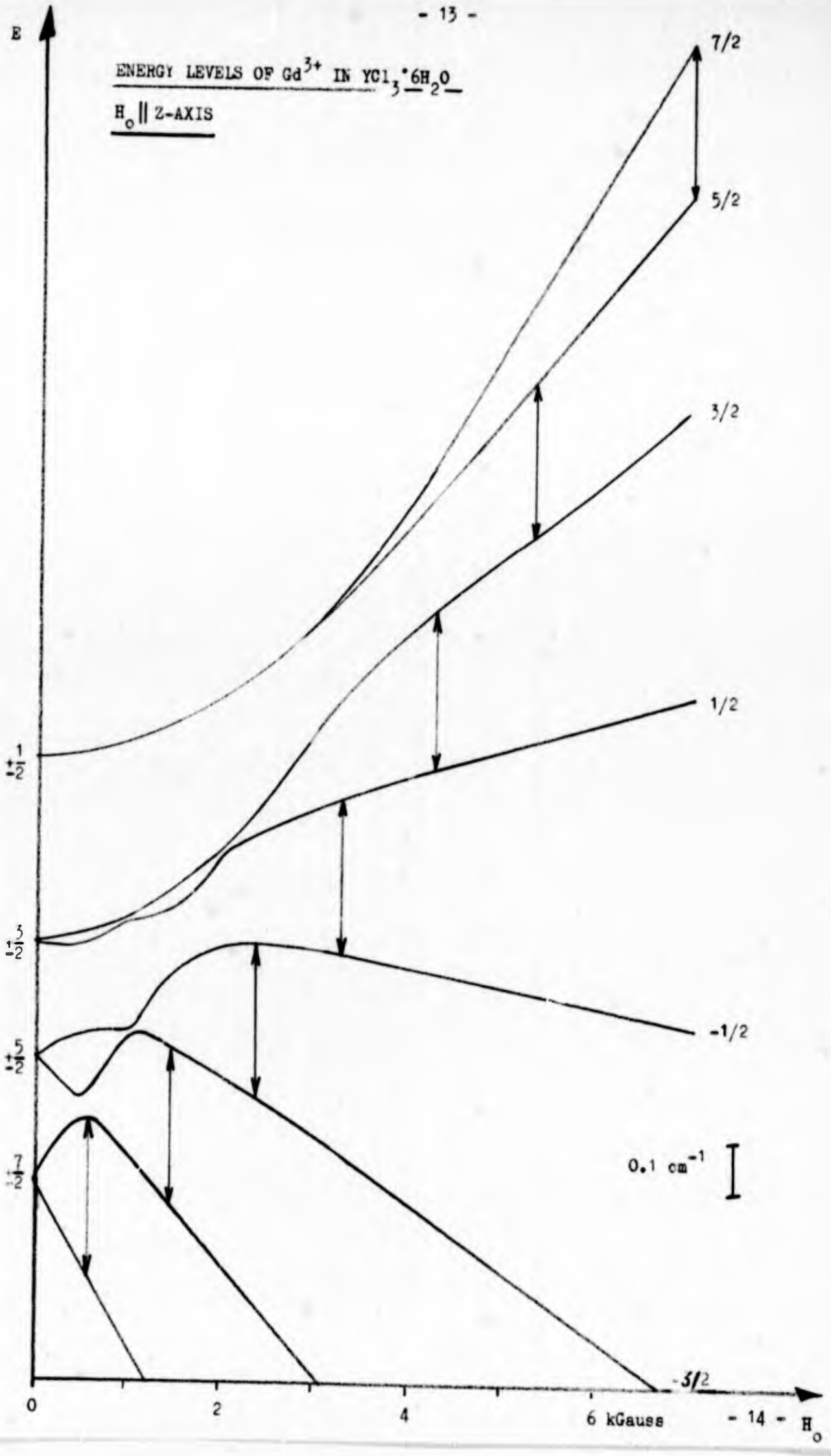
E
ENERGY LEVELS OF Gd^{3+} IN $YCl_3 \cdot 6H_2O$
$H_o \parallel$ Z-AXIS
7/2
5/2
3/2
1/2
-1/2
-3/2
$\pm\frac{1}{2}$
$\pm\frac{3}{2}$
$\pm\frac{5}{2}$
$\pm\frac{7}{2}$
0.1 cm^{-1}
0
2
4
6 kGauss
H_o

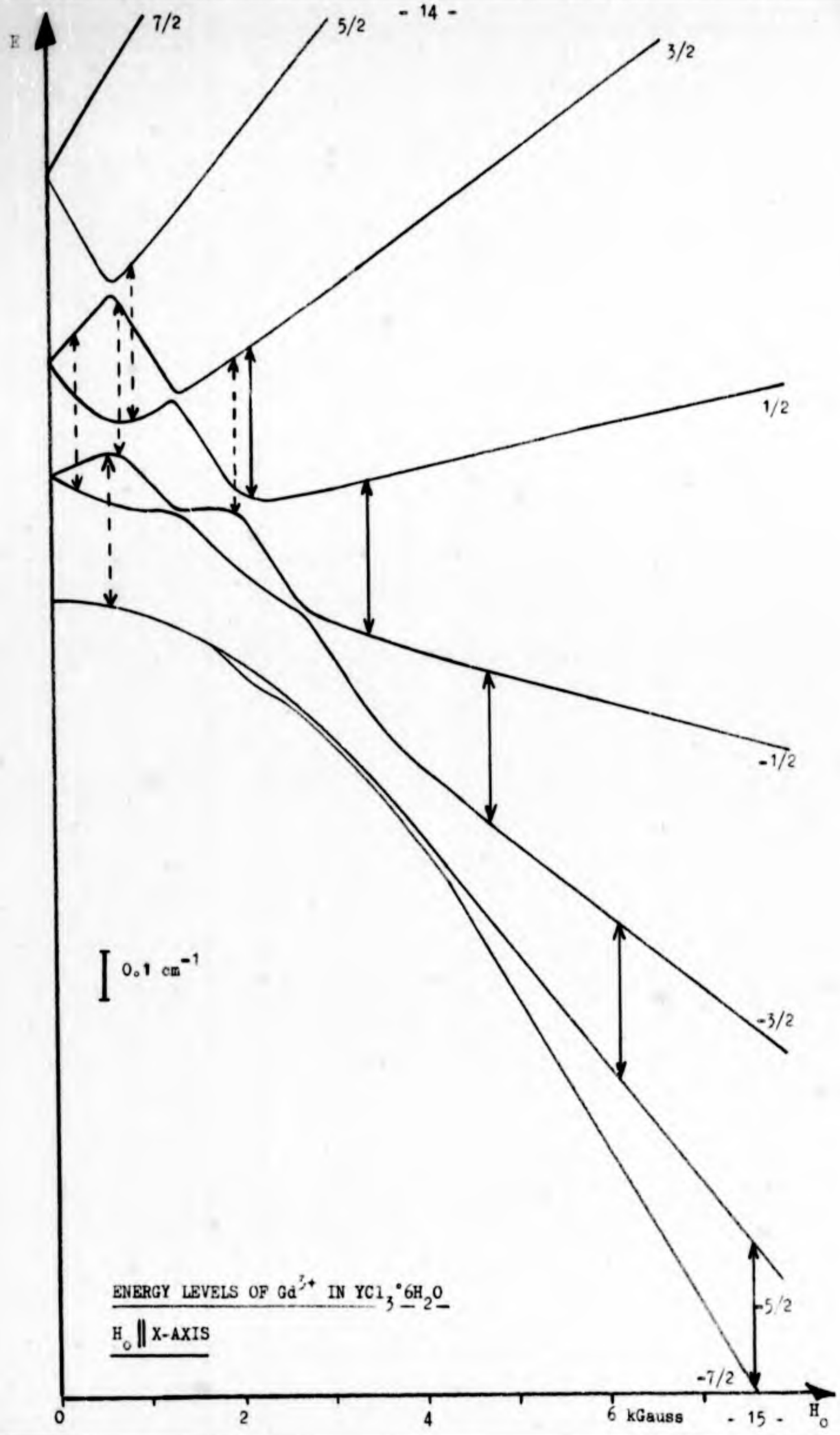

ENERGY LEVELS OF Gd^{3+} IN $YCl_3 \cdot 6H_2O$

$H_0 \parallel$ X-AXIS

C. Investigation of Doped SnO_2 Single Crystals

We got SnO_2 single crystals synthesizing them from the vapor phase [1]. SnO_2-powder was reduced to SnO in a high-Temperature furnace at a temperature of about 1650°C. Nitrogen serving as carrier-gas led the SnO vapor to a zone of lower temperature, where it was reoxidized to SnO_2.

To control this reaction we used a special furnace made by W.C. HERAEUS, whose temperature gradient could be adjusted. The picture shows our experimental set up and the used temperature gradient.

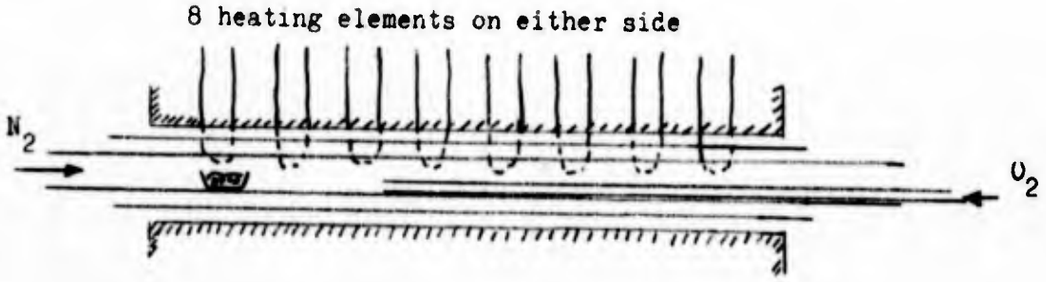

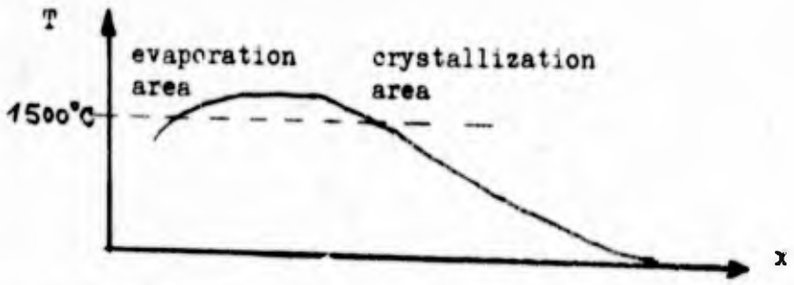

We had varied temperature gradient and supply of N_2 and O_2 so long, till we had got single crystals with a size of about 2x3x15 mm^3. These had no faults and were of excellent optical quality. If we wanted doped crystals, we put a compound of the element to be doped with into a zone of the furnace giving a suitable vaporpressure. The table gives a survey of all crystals we have got.

crystal	colour	size
SnO_2 pure	colouress, transparent	
SnO_2 weakly doped with V^{4+}	yellow	
SnO_2 strongly doped with V^{4+}	yellow-brown	
SnO_2 weakly doped with Fe^{3+}	pink-gray	
SnO_2 strongly doped with Cr^{3+}	violett	about 2x3x15 mm^3
SnO_2 doped with Mn^{4+}	yellow	
SnO_2 weakly doped with Sb^{5+}	light-blue	
SnO_2 strongly doped with Sb^{5+}	dark blue	
SnO_2 doped with Nb^{5+}	dark blue gray	
SnO_2 doped with Ta^{5+}	dark blue gray bluish	

SnO_2 is a semiconductor with an energy gap of 3.52 eV. We could prove this measuring the absorption spectrum and the specific resistivity. Using a LEITZ double beam spectrophotometer we got the transmission of our SnO_2 crystals in the range of λ = 0.3 - 10 μ. Pure SnO_2 crystals are transparent in the range of λ = 0.35 - 1.1 μ as shown by the figure The fundamental edge at λ = 0.3485 μ corresponds to the energy gap.

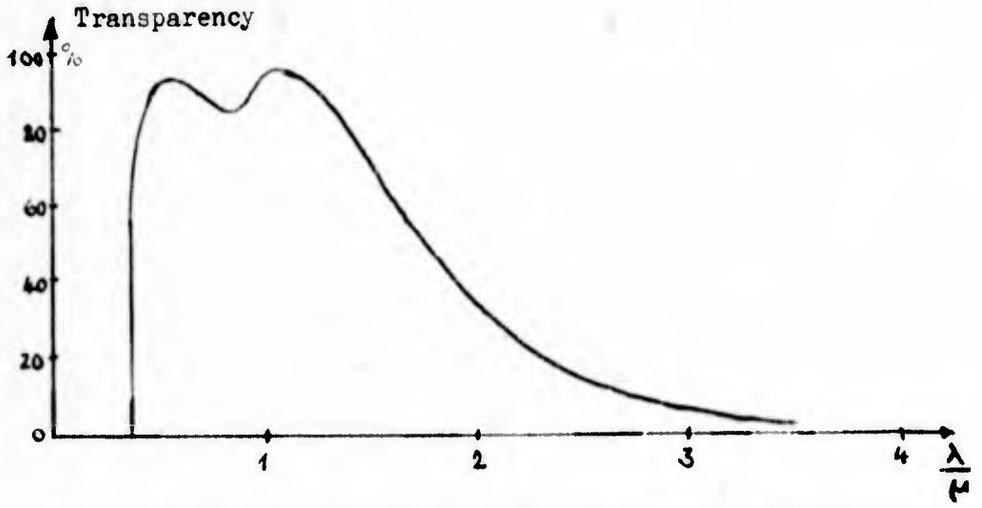

We measured the resisitivity of our SnO_2 crystals using a comparative method: A current is driven by a battery through both, the crystal and a calibrated resistor of similar resistance as the crystal. Measuring the voltages at the resistor and the crystal using a digital voltmeter with an entry impedance greater $10^{10}\Omega$ gives the crystals resistivity R_C:

$$R_c = \frac{U_c}{U} R$$

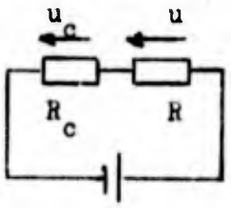

Pure SnO_2 crystals showed no electric conductivity, the specific resistivity was $\varrho \gtrsim 10^6 \Omega$ cm at room temperature.

When we reduced our SnO_2 crystals in a hydrogen atomsphere, they showed stoichiometric impurity conduction. Depending on reduction time and temperature any specific conductivity between $1/\varrho = 10^2 \Omega^{-1} cm^{-1}$ and $10^{-6} \Omega^{-1} cm^{-1}$ could be achieved. The conductivity was growing with increasing temperature:

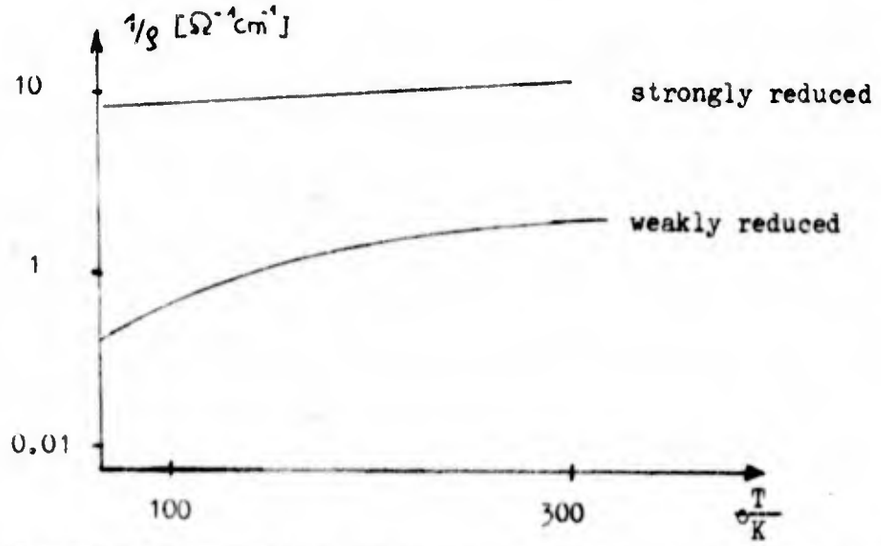

The reduced crystals were bluish. Recording the transmission showed clearly setting in absorption of conduction electrons:

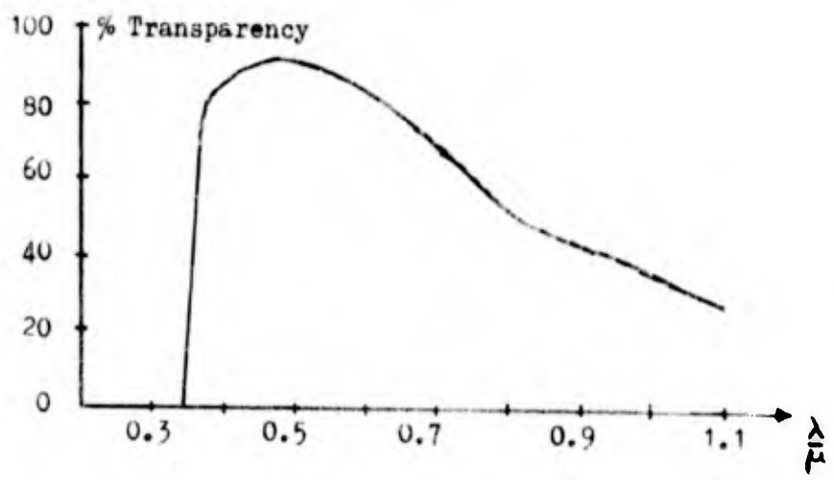

When we doped SnO_2 crystals with Sb, Nb and Ta additional conduction electrons got into the conduction band, because Sb^{5+}, Nb^{5+} and Ta^{5+} ions in SnO_2 form shallow impurity states. Therefore the electric conductivity is strongly increasing. We measured the specific conductivities of such crystals and got the following typical values:

$SnO_2:Sb^{5+}$ $1/\varrho = 600\ 1/\Omega\,cm$
$SnO_2:Nb^{5+}$ $1/\varrho = 120\ 1/\Omega\,cm$
$SnO_2:Ta^{5+}$ $1/\varrho = 18\ 1/\Omega\,cm$

The values depend slightly on growing conditions. Comparing our results with values published elsewhere [2] we got an electron concentration of about 10^{19}-10^{20} $1/cm^3$. The specific resistivity does not depend on temperature over wide ranges, indicating that all the dilute ions have spent an electron upon the conduction band. $SnO_2:Sb^{5+}$, Nb^{5+}, Ta^{5+} crystals are highly degenerated semiconductors.

The optical investigation of SnO_2-crystals doped with shallow impurities delivered principally the same results as the reduced crystals. The figure shows clearly the absorption edge and the absorption by the conduction electrons.

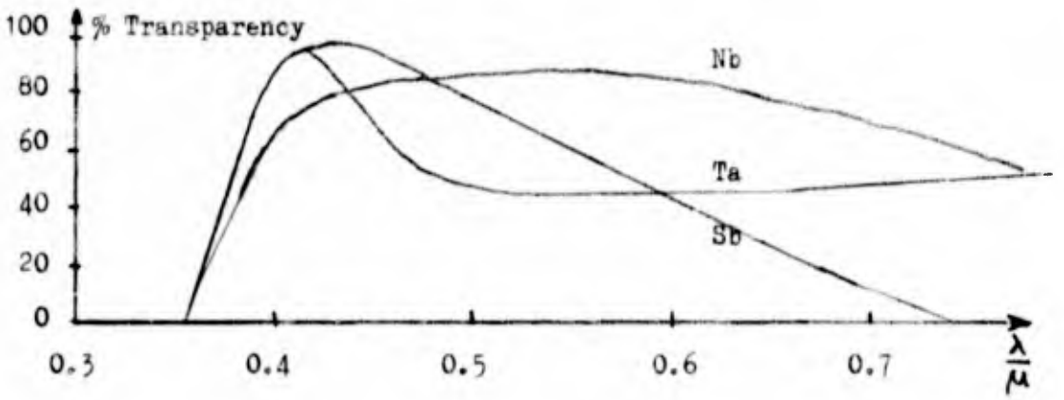

SnO_2:Sb, Nb, Ta crystals showed a single ESR-line according to the conduction electrons. The line-shape of the bigger crystals was asymmetric because of the skin-effect, that of the smaller ones was still symmetric.

SnO_2: Sb_2O_3

1.2 x 1.6 mm^2 0.4 x 0.4 mm^2 0.1 x 0.1 mm^2

cross section of probe

The resonance magnetic field dependends on the angle between magnetic field direction and crystallographic c-axis. It showed the following dependance according to a spin S = 1/2:

$$H_{res} = \frac{H_\perp}{\sqrt{\left[\left(\frac{H_\perp}{H_\parallel}\right)^2 - 1\right]\cos^2\theta + 1}}$$

H_{res} = resonance magnetic field

$H_\perp$ = resonance magnetic field perpendicular to crystallographic c-axis

$H_\parallel$ = resonance magnetic field parallel to crystallographic c-axis

θ = angle between magnetic field and crystallographic c-axis

Comparing the resonance of SnO_2 crystals with a DPPH standard following g-factors were obtained:

$SnO_2:Sb^{5+}$: $g_\parallel = 1.900 \pm 0.005$
$g_\perp = 1.878 \pm 0.005$

$SnO_2:Nb^{5+}$: $g_\parallel = 1.883 \pm 0.005$
$g_\perp = 1.875 \pm 0.005$

$SnO_2:Ta^{5+}$: $g_\parallel = 1.896 \pm 0.005$
$g_\perp = 1.873 \pm 0.005$

As the g-factor is connected with the effective mass by the relation [3]

$$g = 2 - 2\left[\frac{\left(\frac{m}{m^*} - 1\right)}{3\Delta E - 2\lambda}\right]$$

m^* = effective mass
m = electron mass
λ = spin orbit coupling constant of valency band at k=0
ΔE = energy gap

We got the spin orbit-coupling constant using the values [2] for the effective mass $m^* = (0.12 - 0.18)\ m$

$\lambda = (0.1 \pm 0.02)$ eV for Sb^{5+} in SnO_2

Estimating the number of paramagnetic centers using the well known sensitivity of our spectrometer we got the value 5×10^{18} cm^{-3} with an uncertainty of one order of magnitude, thus not fully agreeing with the number of electrons got by resistivity measurements.

We investigated the temperature dependance of the ESR signal in the range of $T = 4.2^{\circ} - 450^{\circ}K$. The intensity obeyed the law

$I \sim T^{-1}$.

The signal could not be saturated with a klystron power of about 160 mW. It did not depend on pressure up to 40 000 N/cm^2 and UV radiation.

Yet we have reported our investigations made on SnO_2 doped with ions forming shallow impurity states. We have also investigated SnO_2: Fe^{3+}, V^{4+}, Cr^{3+}, Mn^{4+} crystals with deep impurity states. These crystals give rise to paramagnetic absorption of localized electrons at the impurity site and to a distinct superhyperfine structure of these electrons with the neighboured Sn nuclei.

We give here a summary of our investigations of SnO_2 doped with Fe^{3+} [4] vicarious for those crystals doped with the other deep impurity states, which showed similar results. SnO_2 has rutile structure and belongs to the space group D_{4h}^{14}, Z = 2 [5]. There are two nonequivalent Sn-sites in the unit cell, which can be carried over by a rotation of 90° round the c-axis.

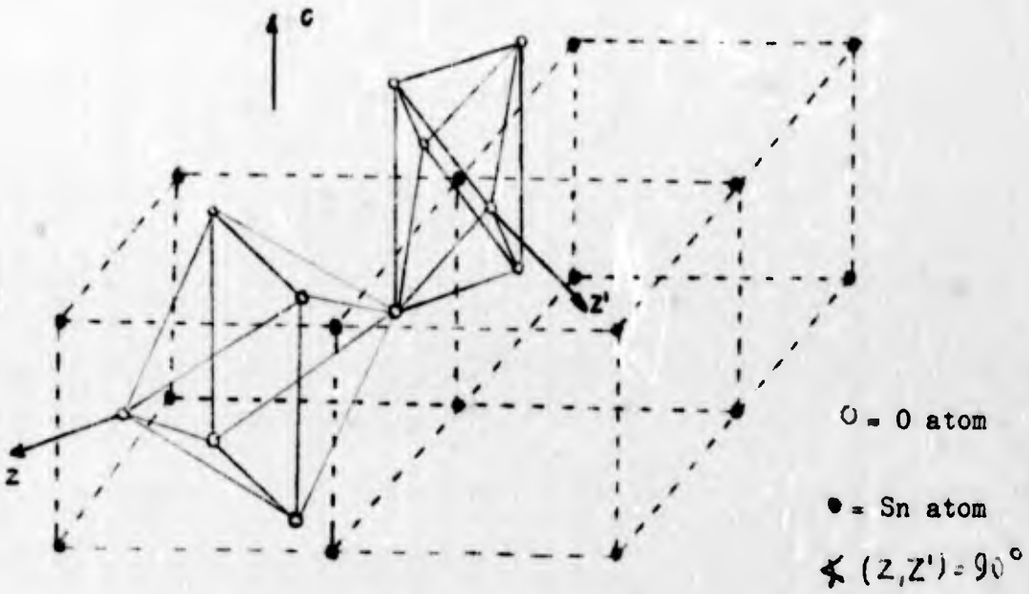

Analyzing the ESR of SnO_2 doped with iron showed two spectra A and B. They could easily be saturated even at room temperature indicating that the paramagnetic centers are only weakly coupled to the lattice. We attach spectrum A to iron ions sitting on a lattice site, because it is symmetric in the (001)-plane to the bisectrix between the two nonequivalent lattice sites. Spectrum B belongs to Fe^{3+} on an interstitial site.

To describe spectrum A we used the following Hamiltonian

$$H = \beta \vec{H}_o \tilde{g} \vec{S} + D \left(S_z^2 - \tfrac{1}{3}S(S+1)\right) + E \left(S_x^2 - S_y^2\right)$$

according to the ortho-rhombic surrounding of the iron ions.

We got the following values for the constants D and E

$g = 2$

$|D| = (0.681 \pm 0.005)\ cm^{-1}$

$|E| = (0.072 \pm 0.005)\ cm^{-1}$

The signs of D and E could not yet be determined, because hitherto no signals could be achieved at liquid helium temperature. The signal had been saturated at once. These constants nearly agree with those of $TiO_2:Fe^{3+}$, because the dimensions of either elementary cell are the same [6].

Using these parameters we could compute the angular variation of spectrum A with an accuracy of 2.5% with respect to the experimental results. The variation of energy versus magnetic field is given on page 25. The arrows mark the klystron frequencies. We used wavelengths at 3 cm and 8 mm.

The zero field splittings are rather large compared with other Fe-doped crystals. Besides one exception we could only observe transitions between single Kramers doublets even in the Q-band. Therefore we had not enough data for our program to compute further terms of the Spin-Hamiltonian. So the parameters a and F were neglected.

We attach spectrum B to Fe^{3+} ions on interstitial sites in the middle of the (100) plane and the $[\bar{1}00]$ edges. We could only observe transitions between the single Kramers-doublets, so we assume that the zero field splittings are still larger than those of spectrum A. From the angular variation we estimate the value of D of spectrum B about $|D| \approx 0.72\ cm^{-1}$. All lines of spectrum B are split twice and are separated by an amount of $\delta \approx 1$ gauss. We could not yet explain this behaviour, but we believe that there may be two potential troughs at the interstitial site.

Both, spectrum A and B showed further splitting of the ESR lines according to interaction IAS of the paramagnetic centers with the magnetic Sn^{115} and Sn^{117} nuclei (I = 1/2), which have an natural abundance of ...16%. Each Fe^{3+} ion on a lattice

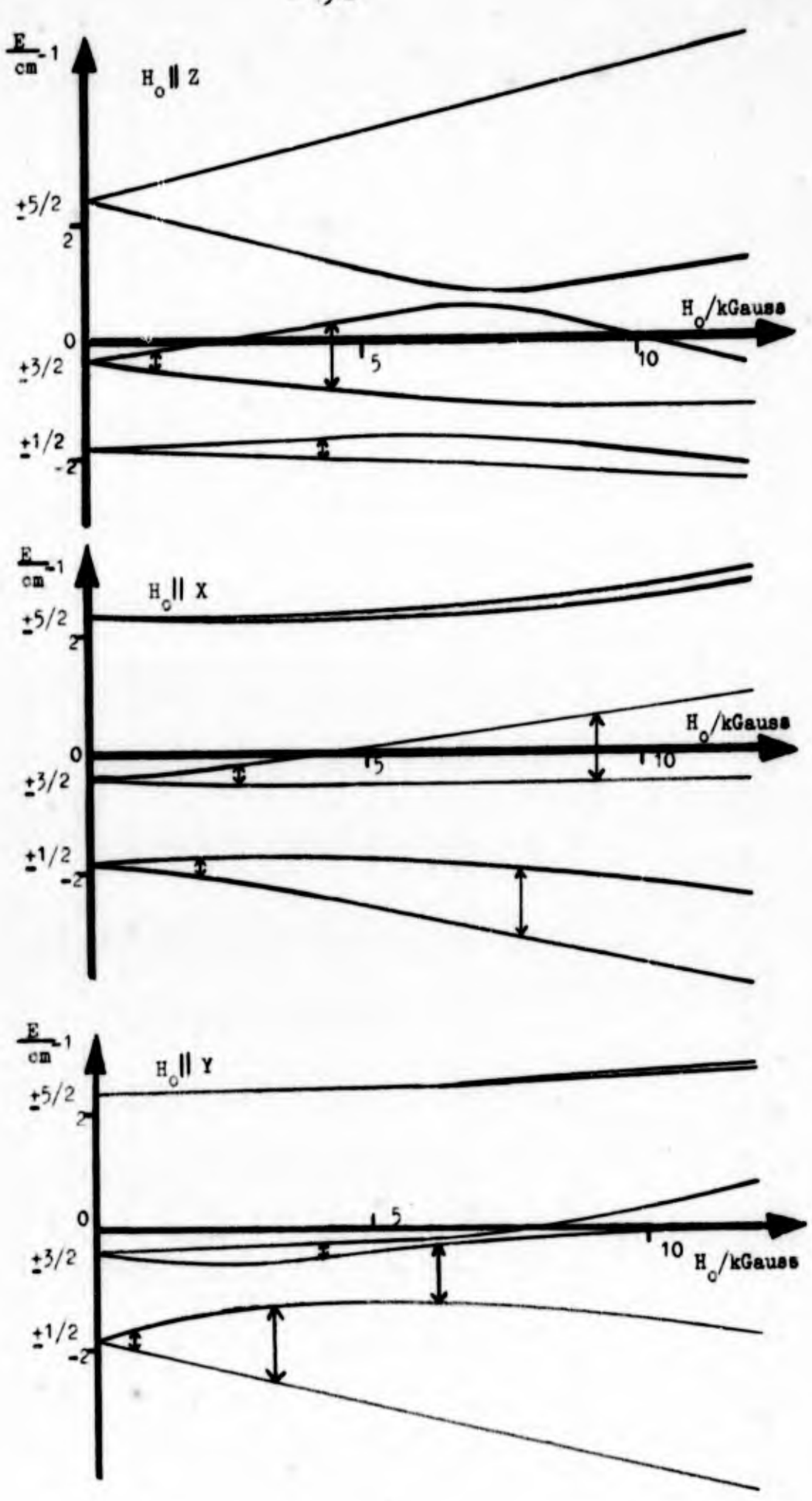

ENERGY LEVELS OF Fe^{3+} IN SnO_2 AND THE TRANSITIONS AT 3cm and 8mm

site is surrounded by ten tin-nuclei. The distance to both the nuclei on the c-axis is smaller than that to the other eight. This gives rise to two different super-hyperfine interactions $S\tilde{A}^{(2)}I$ and $S\tilde{A}^{(8)}I$ of the iron ion with two and eight tin nuclei.

Coupling of Fe^{3+} to the two next Sn-nuclei gives rise to splitting into five lines. Each of these splits furthermore into seventeen lines because of the interaction with the eight Sn-nuclei second nearest neighboured. Thus, 85-fold splitting is to be observed, but we could only resolve a 13-fold one in the best case. The other lines were masked by the linewidth.

Observing the ESR spectrum A in the direction of the c-axis we got the following values for the coupling constants

$A_y^{(2)} = (6.92 \pm 0.05)$ gauss
$A_y^{(8)} = (4.78 \pm 0.05)$ gauss

In the other two main directions we got the values

$A_x^{(2)} = A_x^{(8)} = (5.0 \pm 0.6)$ gauss
$A_z(2) = A_z^{(8)} = (4.2 \pm 0.2)$ gauss

In the case of Fe^{3+} on an interstitial site a super-hyperfine structure had been observed, too. Fe^{3+} is here surrounded by six Sn-nuclei giving rise to a 13-fold splitting, but we could not all observe because of the linewidth. We determined the coupling constant C_y in the direction of the crystallographic c-axis

$C_y = (5.6 \pm 0.8)$ gauss.

Our investigation of super-hyperfine structure of $SnO_2:Ti^{3+}$ showed the dominating rule of covalence bounding of the Fe^{3+} ion.

1) J.A. Marley et al., J. Appl. Phys. 32, 2504 (1961)
2) J.A. Marley et al., Phys. Rev. 140 A, 304 (1965)
3) L.M. Roth, Phys. Rev. 118, 1534 (1960)
4) G. Sperlich, to be published
5) S.L. Hou et al., Phys. Rev. 154, 258 (1967)
6) D.L. Carter et al., Phys. Rev. 118, 1485 (1960)

D. Fluorescence Lifetime Measurements of Ruby

We have already reported our lifetime measurements of ruby [1,2] using a set up according to Zarowin [3]. Our crystals had been grown by the Verneuil technique [4]. We got Al_2O_3 single crystals doped with chromium concentrations of 0.05% - 1% depending on the concentration of the starting materials. They were suitable to observe the fluorescence of the single Cr-ions and the additional fluorescence of Cr-Cr pairs. The lifetime had been measured by a sampling technique registring single photons.

We could confirm the results of Imbusch [5]. Because the pair lines showed nearly the same lifetime as the single ions a radiationless energy transfer is assumed from the metastable ^2E levels of the single ions to the metastable levels of the pairs.

1) Our Progress Report NO. 3, 22nd July 1966
2) Our Scientific Report NO. 1, March 1967
3) C.B. Zarowin, Rev. Sci. Inst. , 1051 (1963)
4) Our Progress Report NO. 1, 22nd July 1965
5) G.F. Imbusch, IEEE J. Quant. , QE-2, 532 (1966)

E. Some of our Investigations of Boracites

Some of our measurements of boracites have already been reported [1] in detail. We measured the optical absorption [2,3] and the paramagnetic absorption [4]. Furthermore we could achieve frequency doubling [5,6] and measure the pyro- and magneto-electric effect (p.p 29).

Boracites are crystals with the chemical sum-formula $Me_3^{2+}B_7O_{13}X$ (Me=metal, X=halogen). Natural Boracite (Stassfurtith) has the formula $Mg_3B_7O_{13}Cl$ and is found near Stassfurt (DDR). We have got several artificial boracites growing them with aid of a transport-reaction according to H. Schmid [7]:

$$7\ B_2O_3 + MeX_2 + 5\ MeX_2 + 5\ H_2O \longrightarrow 2\ Me_3B_7O_{13}X + 10\ HX$$

$$5\ MeO + 10\ HX \qquad 5\ MeX_2 + 5\ H_2O$$

The reaction takes place in a quartz-vessel at a temperature of about 900 °C during several hours. We got Ni-Cl, Ni-J, Cd-Cl, Cd-J, Fe-Cl and Zn-Cl boracites with an average size of 20 mm^3. Zn-Cl boracites have been got putting the quartz vessel in an autoclave, in which a pressure of about 10 atm was to prevent bursting of the ampoule.

We investigated boracites, because they allowed to change easily the diamagnetic surrounding of a transition-metal ion by changing the halogen atoms. Furthermore boracites show some interesting effects because of their low symmetry (C_{2v}^5) in their low temperature-phase, which mostly exists already at room temperature. Thus, ferroelectricity, weak ferromagnetism, the pyroelectric effect, the magnetoelectric effect and frequency doubling could be observed.

We have recorded and interpreted the optical absorption of Ni-Cl, Ni-J and Fe-Cl boracites in the range 350nm-19 μ at room temperature and the temperatures of liquid nitrogen and helium. We found that all absorptions from 3.5 μ to shorter wavelengths were due to electronic transitions. We have interpreted these as transitions of single transition-metal ions in tetragonal surrounding using the crystal field theory of Tanabe and Sugano [8].

From our spectra we got fits for the Coulomb parameters B and C, the cubic crystal-field splitting parameter Dq and the tetragonal crystal-field splitting parameters δ and Δ :

	B	C/B	Dq	δ	Δ/δ
Ni-J	875 cm^{-1}	3.74	675 cm^{-1}	2500 cm^{-1}	0.86
Ni-Cl	875 cm^{-1}	4.1	620 cm^{-1}	2200 cm^{-1}	0.86

Because not all transitions could be coordinated, we could only estimate the following data for the Fe-Cl boracite.

$10\ Dq + \delta/2 = 11000\ cm^{-1}$; $\Delta, \delta \approx 3000\ cm^{-1}$

Computing the energy niveaus of the corresponding metal ions with these constants a good agreement with our measurements was only found for the lower energies. Covalency may be responsible for the deviations at higher energies.

Recording the spectrum of Ni-Cl boracite with high resolution we have found a fine structure of the absorption bands. This consists of steps of about 100 cm^{-1} which may be attributed to the energy of a phonon.

When we investigated the ESR of Cd-Cl and Cd-J boracites doped with nickel we found three absorption lines. We attach these to Ni^{2+} ions sitting on three nonequivalent lattice sites [8]. Though Ni^{2+} has a spin S = 1 the zero field splitting in the tetragonal surrounding of a Ni^{2+} ion seems to be so large that only transitions can be observed between the doublet lying lowest. Thus we could describe each absorption line by an effective spin $S_{eff} = 1/2$. The angular variation of each line was described by the formula

$$H = \frac{H_\perp}{\sqrt{\left[\left(\frac{H_\perp}{H_\parallel}\right)^2 - 1\right]\cos^2\varphi + 1}}$$

and the following values for the g-factors were achieved

	$g_\parallel$	$g_\perp$
Cd-Cl : Ni^{2+} Boracite	2.552	2.113
Cd-J : Ni^{2+} Boracite	2.590	2.110

Frequency doubling on boracites was obtained using a self-built Nd-glass LASER with rotating prism. This delivers a single pulse with a half-width of 50 nsec and a maximum energy of 200 mJ.

Mg-Cl, Cd-Cl, Zn-Cl, Cd-J boracites showed frequency doubling which could be seen with the naked eye. It is more intensive than that of quartz. Fe-Cl boracite shows only weak frequency doubling because of its optical absorption. Ni-J boracite shows no frequency doubling because it is in the cubic phase at room temperature. Furthermore it is nearly non transparent.

The here summarized investigations of boracites have not yet been finished. They turn out lengthy because we have only small crystals, so that measurements are troublesome.
Furthermore interpreting of data is difficult, as the elementary cell of boracite is very complicated. It contains 96 atoms.

1) Our Scientific Report No. 1, 1th March 1967 (summary)
2) Our Progress Report No. 3, 22nd July 1966 (optical absorption measurements)
3) Our Progress Report No. 6 and 7, 14th December 1967 (optical absorption measurements)
4) Our Progress Report No. 2, 7th April 1966 (ESR measurements)
5) Our Progress Report No. 4, 2nd December 1966 (frequency doubling)
6) Our Progress Report No. 5, 1st June 1967 (frequency doubling)
7) H. Schmid, J.Phys.Chem.Sol. 26,973 (1965)
8) Y. Tanabe et al., J.Phys.Soc.Jap. 9, 753, 766 (1954)
9) T.Ito et al., Acta cryst. 4,310 (1951)

F) Magneto-Electric Effect of Ni-J Boracite

All boracites show a cubic high temperature phase (α-phase) and an orthorhombic low temperature phase (β-phase). The conversion point varies from 64 °K to 800 °K depending on the special type of boracite. Contrary to the other boracites Ni-JB becomes antiferromagnetic at 120 °K already and below 64 °K it becomes weak ferromagnetic. At this temperature the conversion from the high to the low temperature phase takes place as well as the transition from the piezoelectric to the ferroelectric state. Below 64 °K both ferromagnetic and ferroelectric domains can exist.

Our measurements were made with the aim to study the magneto-electric effect MEE and nonlinearities of the magneto-electric polarization as well as the pyroelectric effect PEE of Ni-JB.

The equations of the MEE and PEE are related to the thermodynamic potential

$$\phi = F + \sum_{i,k} \alpha_{ik} E_i H_k - \vec{E}\vec{D}' - \vec{H}\vec{B}'$$

F = Helmholtz free energy, α_{ik} = magneto-electric coefficients. Differentiating ϕ one obtains:

$$D = - \frac{\partial \phi}{\partial E}_{T, H = \text{const.}} \qquad B = - \frac{\partial \phi}{\partial H}_{T, E = \text{const.}}$$

The potential function is restricted to the magnetic symmetry of the crystal thus reducing the independent coefficients.

The point symmetry of Ni-JB in the low temperature phase is mm2. The possible magnetic symmetries are m m 2; $\underline{m}$ $\underline{m}$ 2; and $\underline{m}$ m $\underline{2}$. [1]. m m 2 is not allowed because ferromagnetism in this point group does not exist. $\underline{m}$ $\underline{m}$ 2 allows a magnetization along the two-fold z-axis, this was not observed [2]. The point group $\underline{m}$ m $\underline{2}$ gives rise to a spontaneous magnetization.

With respect to the symmetry m m 2 the ϕ function for the MEE of Ni-JB in the β-phase can be written:

$$\phi = \phi_0 - \frac{1}{2}\left[\varepsilon_x E_x^2 + \varepsilon_y E_y^2 + \varepsilon_z E_z^2 + \mu_x H_x^2 + \mu_y H_y^2 + \mu_z H_z^2\right] - \left[\alpha_{yz} E_y H_z + \alpha_{zy} E_z H_y\right]$$

ε_i = ordinary dielectric constants, μ_i = ordinary permeabilities, and α_{ik} = magneto-electric coefficients.

Differentiating ϕ one obtains the components of $\vec{D}$ and $\vec{B}$:

$$\vec{D} = (\varepsilon_x E_x,\ \varepsilon_y E_y + \alpha_{yz} H_z,\ \varepsilon_z E_z + \alpha_{zy} H_y)$$

$$\vec{B} = (\mu_x H_x,\ \mu_y H_y + \alpha_{zy} E_z,\ \mu_z H_z + \alpha_{yz} E_y)$$

The magneto-electric polarization is

$$\vec{P} = (0,\ \alpha_{yz} H_z,\ \alpha_{zy} H_y)$$

The magneto-electric magnetization is

$$\vec{M} = (0,\ \alpha_{zy} E_z,\ \alpha_{yz} E_y)$$

For the measurements of the MEE disks parallel to a (100) plane were needed which contained only one domain. Therefore carefully selected crystals were cut parallel to a natural (100) plane. The orientation could be easily checked with the aid of a polarization microscope. A dark cross can be seen if the axes of two crossed polarizators are aligned parallel to the [110] direction and to the [1$\bar{1}$0] direction respectively. The small arms of the cross connect the (111) A planes while the broad arms direct to the (111) B planes. The next two figures show the orientation of the boracite crystal.

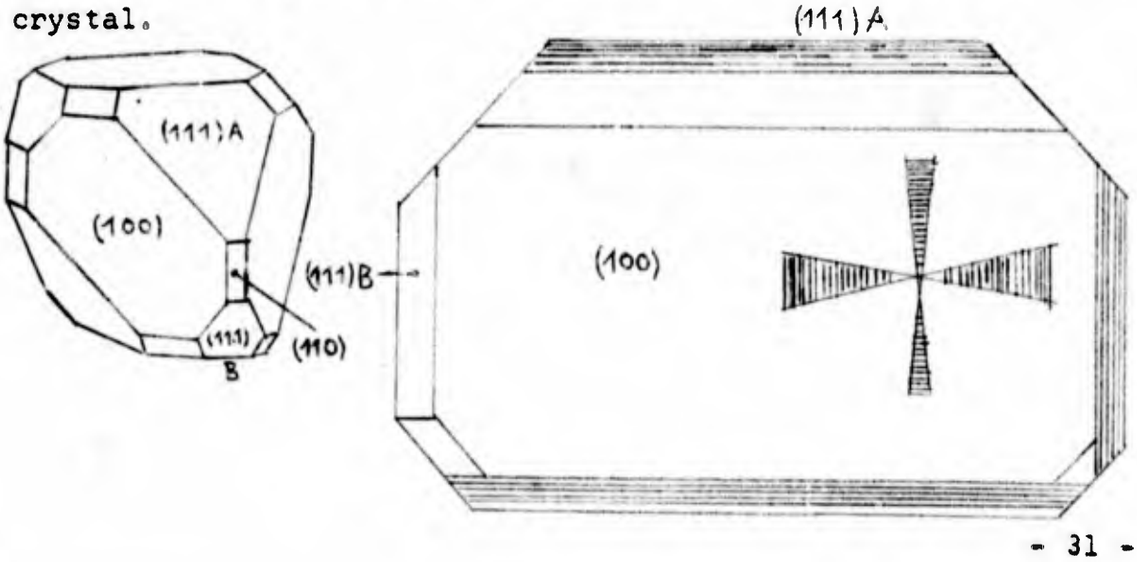

The crystals were polished to a thickness of about 0.1 mm and mounted on a special probe which is shown in the next picture.

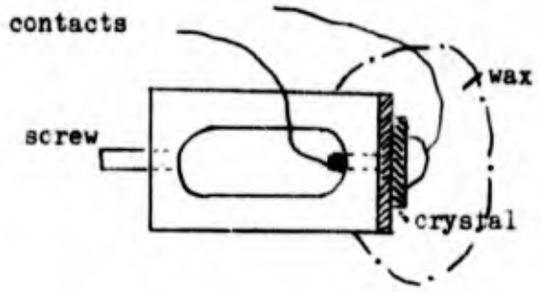

Fig. Probe for MEE and PEE measurements

The (100) planes of the crystal disk were contacted. An electric field of 10 kV/cm was applied parallel to the [100] direction while a magnetic field of 10 kOe was applied parallel to the [110] direction. The crystals had been cooled to 20 ^{o}K to get only one ferromagnetic ferroelectric domain. To determine the magneto-electric coefficients α_{yz} and α_{zy} we measured P_y and P_z using a Cary electrometer. P_y was too small to be measured with our set up, so we could determine only $P_z = \alpha_{zy} H_y$. During the measurement of the polarization caused by a magnetic field the temperature had to be constant, because of the PEE, for a change in temperature ΔT caused an additional polarization $\Delta P = q \Delta T$ (q = pyroelectric coefficient).

The pyroelectric coefficient q depends strongly on temperature, at 60 ^{o}K it is about $0.5 \cdot 10^{-6}$ $As/m^2 \cdot {}^{o}K$. At lower temperatures q decreases. The pyroelectric polarization of Ni-JB versus temperature is shown on the next picture. The pyroelectric polarization has a maximum at the transition point from the low temperature phase to the high temperature phase at 64 ^{o}K (indicated by an arrow). On account of the strong PEE Ni-JB seems to be a suitable thermometer material. The pyroelectric voltage $U = q \cdot (A/C) \cdot T$, A is the area of the crystal, C is the capacity, and T the temperature, is about four orders of magnitude greater than the thermoelectric voltage of ordinary thermoelements. There is, however, the disadvantage that a magnetic and an electric field must be applied to get a single ferromagnetic ferroelectric domain.

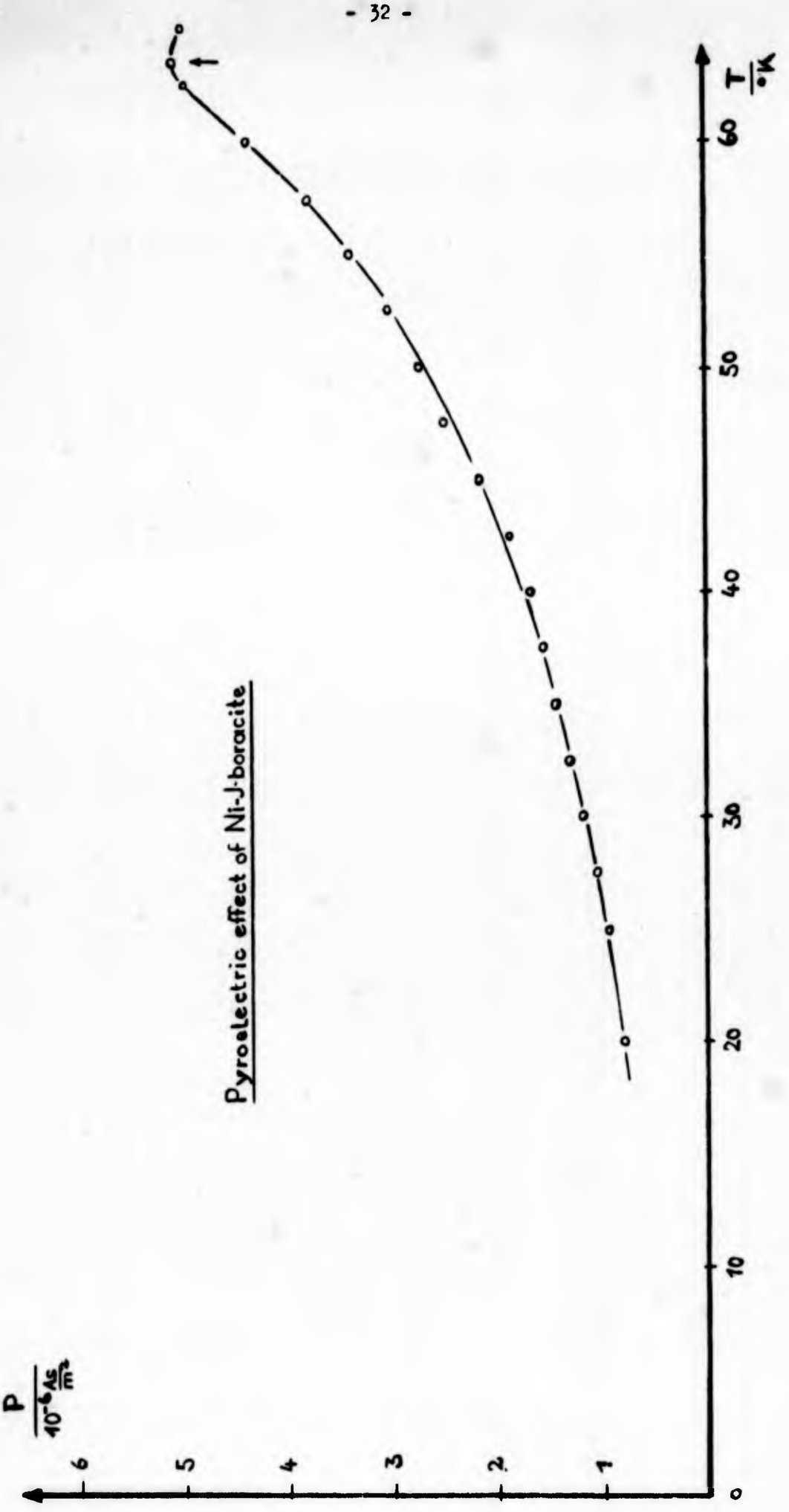

Pyroelectric effect of Ni-J-boracite

The magneto-electric polarization is shown on the next figure. A "butterfly" curve is obtained for P_z versus H. The magneto-electric coefficient $\alpha_{zy}(H=0)$ is $6.45 \cdot 10^{-12}$ sec/m.

---

1) Birss, R. R., Magnetism and Symmetry, NHPC, (64)

2) Schmid, H., Proceedings of the Symp. on Crystal Growth, Moscow, July 1966

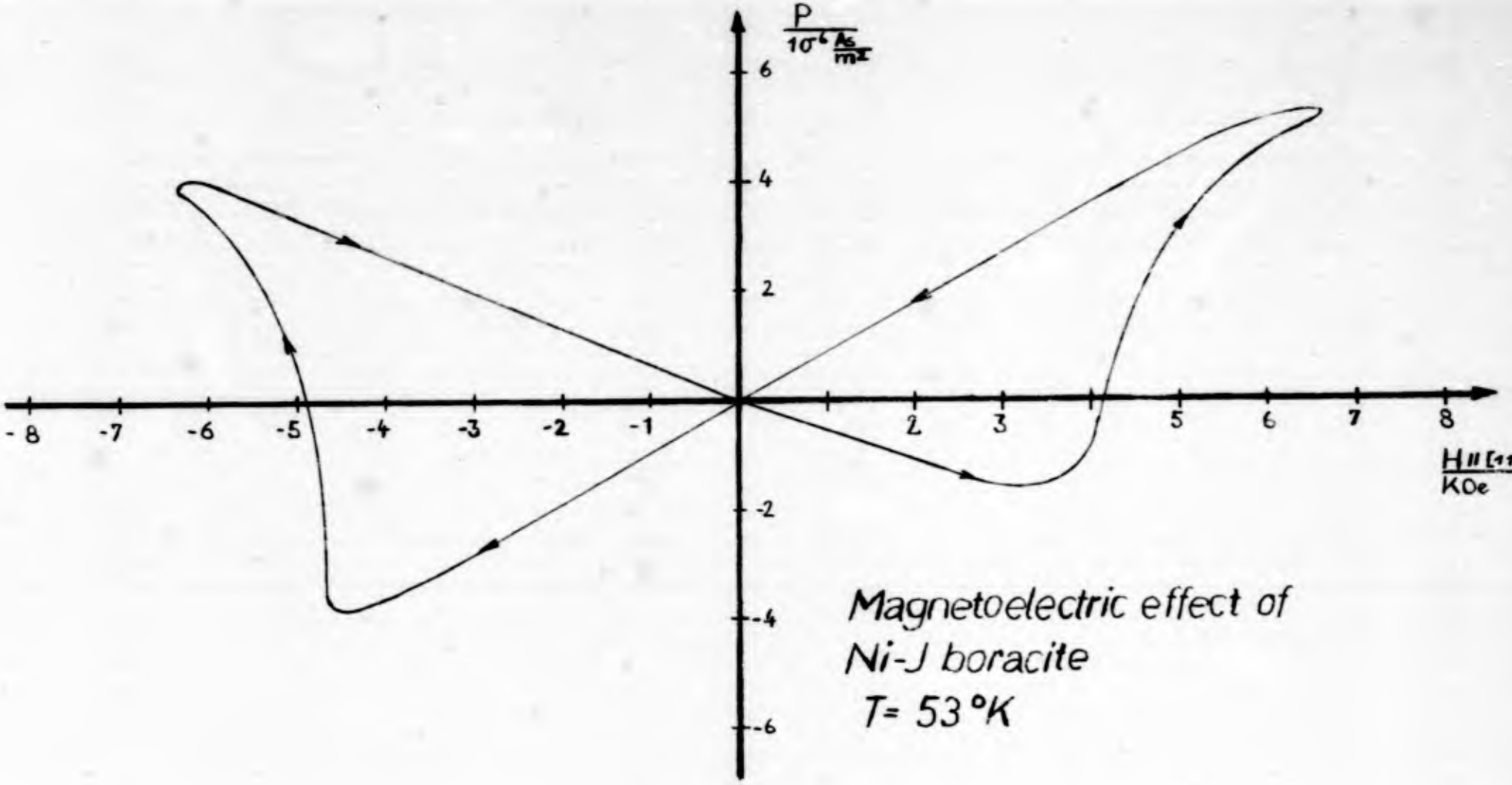

Magnetoelectric effect of
Ni-J boracite
T= 53 °K

UNCLASSIFIED

Security Classification

DOCUMENT CONTROL DATA - R & D

(Security classification of title, body of abstract and indexing annotation must be entered when the overall report is classified)

1. ORIGINATING ACTIVITY (Corporate author)

Physikalisches Institut
Technische Hochschule Darmstadt
6100 Darmstadt, Germany

2a. REPORT SECURITY CLASSIFICATION: Unclassified

2b. GROUP:

3. REPORT TITLE

INVESTIGATIONS OF SOME OXIDE CRYSTALS BY ESR AND OPTICAL METHODS

4. DESCRIPTIVE NOTES (Type of report and inclusive dates): Scientific. Report.

5. AUTHOR(S) (First name, middle initial, last name)

B. Elschner

6. REPORT DATE: 1 Sep 68

7a. TOTAL NO. OF PAGES: 33

7b. NO. OF REFS: 2

8a. CONTRACT OR GRANT NO: AF61(052)-817

b. PROJECT NO: 4645-02

c. 62405314

d. 6813

9a. ORIGINATOR'S REPORT NUMBER(S):

9b. OTHER REPORT NO(S) (Any other numbers that may be assigned this report):

10. DISTRIBUTION STATEMENT

This document has been approved for public release and sale; its distribution is unlimited.

11. SUPPLEMENTARY NOTES:

12. SPONSORING MILITARY ACTIVITY: Air Force Cambridge Research Laboratories (CRO)L.G.Hanscom Fld, Bedford, Mass. 01730

13. ABSTRACT

The mineral Benitoitewas investigated by Electron-Spin-Resonance (ESR)[7]. We have written a FORTRAN-Program to compute the constants of the Spin-Hamiltonian from the resonance magnetic fields. It also computes the energy eigenvalues of the Spin-Hamiltonian. These are in good agreement with experiment thus indicating that the right Spin-Hamiltonian was chosen.

This program was used to set up the Spin-Hamiltonian of gadolinium ions Gd^{3+} in $YCl_3 \cdot 6\ H_2O$ and of iron ions Fe^{3+} in SnO_2.

SnO_2-crystals, both undoped and doped with vanadium ions V^{4+} and iron ions Fe^{3+}, were grown from the vapor phase and investigated by measuring resistivity, optical transmission, and ESR.

Ruby-crystals with different concentrations of chromium ions Cr^{3+} were grown with aid of a Verneuil set up. The fluorescence lifetime was measured at various temperatures and concentrations using a sampling technique according to Zarowin.

Several crystals of the boracite-type were grown with aid of a transport-reaction according to H. Schmid and the optical transmission was analyzed. The ESR-Spectrum of Ni-J-boracite was recorded and interpreted by an effective spin $S_{eff}=1/2$.

A giant pulse LASER was built and frequency doubling of boracites was investigated.

The magneto-electric effect of Ni-J-Boracite has been measured.

DD FORM 1 NOV 65 1473

UNCLASSIFIED

Security Classification